**Supporting Information**

## Intact polar lipid structural assignment

*Sialic acid glycosphingolipid (sGSL)*

Accurate mass determination by Fourier-transform ion cyclotron resonance mass spectrometry (FT-ICR-MS) yielded m/z 870.66535 for the most abundant sGSL species, predicting a formula of $C_{49}H_{92}O_{11}N^+$ ($\delta$ = -1.308 ppm) in positive ion mode. Ion trap $MS^2$ fragment analysis indicated a 268 Da headgroup, C22:0 fatty acid, and d18:2 LCB (Fig. S1). In FT-ICR-MS positive ion mode, the primary $MS^2$ ceramide ion with m/z 620.59733 resulted from a neutral fragment loss of 250.06802 Da ($C_9H_{14}O_8$) and the m/z 602.58694 ion resulted from a neutral fragment loss of 268.07841 Da, pointing to a $C_9H_{16}O_9$ headgroup (Fig. S1). In negative ion mode, sGSL yielded a m/z 249.06135 $MS^2$ fragment ion, which corresponded to the 250.06802 Da neutral fragment loss in positive ion mode, and its $MS^3$ spectrum included two product ions with m/z 129.01923 and m/z 87.00870, supporting the chemical formulas $C_5H_5O_4^-$ and $C_3H_3O_3^-$, respectively (Fig. S2). KDN, which is the deaminated form of N-Acetylneuraminc acid (Neu5Ac), also has the formula $C_9H_{16}O_9$ (Inoue and Kitajima, 2006). The FT-ICR-MS negative ion mode $MS^2$ spectrum for pure KDN (Sigma-Aldrich, ≥99.0%) included m/z 249.06149, 129.01923 and 87.00864 fragment ions that had the same masses as observed in the $MS^3$ spectrum of sGSL (Fig. S3). As with sGSL, the m/z 249.06149 $MS^2$ KDN ion fragmented to yield an $MS^3$ product ion with m/z 129.01922, supporting our interpretation that the headgroup is indeed KDN. We also detected a second sGSL species with m/z 872.68399 ($C_{49}H_{94}O_{11}N^+$; $\delta$ = 2.121 ppm), distinguished by

having a d18:1 LCB instead of the more common d18:2 LCB, and both species were only observed to have C22:0 fatty acids.

*Phosphatidyldimethylpropanethiol (PDPT)*

We detected a series of peaks with m/z 795, 823, 849 and 895 that each yielded m/z 201 ion trap $MS^2$ product ions. The pattern was similar to that of that of phosphatidylcholine ( PC), which had m/z 778, 806, 832 and 878, except that the PC molecular ions yielded m/z 184 $MS^2$ product ions, demonstrating that like PC, the newly identified compound was a polar diacylglycerolipid and had the same fatty acid distributions of [14:0/22:6], [16:0/22:6], [18:1/22:6] and [22:6/22:6], respectively. FT-ICR-MS yielded m/z 795.50051 for the most abundant molecular ion, predicting the formula $C_{44}H_{76}O_8PS^+$ ($\delta$ = 1.517 ppm); thus the new lipid was a phospholipid and contained sulfur. The headgroup $MS^2$ ion had m/z 201.03464, which supports the formula $C_5H_{14}O_4PS^+$ ($\delta$ = 0.733 ppm). Our preliminary structural assignment based on ion trap $MS^n$ fragmentation compared with that of phosphatidylsulfocholine (PSC) suggested that it was phosphatidyldimethylpropanethiol (PDPT), similar to PSC, but with the terminal dimethyl sulfide moiety bound to phosphate via propanol instead of ethanol.

*Betaine-like lipid (BLL)*

We detected a series of peaks with m/z 802, 830, 856 and 902 that each yielded m/z 190 ion trap ms2 product ions, a similar pattern to PC, PDPT and DGCC, and all contained the same fatty acid combinations (Table S2). FT-ICR-MS analysis yielded a molecular ion of m/z 856.59232 for the abundant species, which predicted the formula $C_{50}H_{82}O_{10}N^+$ ($\delta$ = -1.172 ppm). The

headgroup $MS^2$ ion had m/z 190.07098, which supports the formula $C_7H_{12}O_5N^+$ ($\delta$ = -0.100 ppm). Ion trap $MS^n$ fragment analysis suggested the headgroup included amine, carboxyl, and hydroxyl moieties on an n-hexene or pentene backbone. This is similar to the betaine lipids, but there was no ion or neutral fragment associated with trimethylamine. Having the similar requirement of reduced nitrogen without phosphate, we classified this lipid as a betaine-like lipid (BLL).

Table S1. Increasing lipids in infected *Ehux374*

| | C(0)[a] | C(1)[a] | C(2)[a] | C(3)[a] | C(4)[a] | Equation | $R^2$ |
|---|---|---|---|---|---|---|---|
| vGSL | tr.[b] | 0.04 ± 0.01 | 0.33 ± 0.09 | 0.68 ± 0.07 | 1.58 ± 0.32 | $C(t)=0.013e^{1.29t}$ | 0.96 |
| sGSL | 0.09 ± 0.02 | 0.12 ± 0.01 | 0.09 ± 0.04 | 0.22 ± 0.01 | 0.42 ± 0.30 | $C(t)=0.073e^{0.37t}$ | 0.76 |
| PE | 0.02 ± 0.00 | 0.02 ± 0.00 | 0.05 ± 0.01 | 0.21 ± 0.03 | 0.79 ± 0.23 | $C(t)=0.013e^{0.94t}$ | 0.88 |
| DGTS | 0.07 ± 0.01 | 0.09 ± 0.00 | 0.14 ± 0.03 | 0.26 ± 0.02 | 0.37 ± 0.10 | $C(t)=0.064e^{0.43t}$ | 0.97 |
| BLL [22:6/22:6] | tr.[b] | tr.[b] | 0.01 ± 0.00 | 0.03 ± 0.01 | 0.04 ± 0.02 | $C(t)=0.001e^{1.09t}$ | 0.90 |

[a] 0 DPI to 4 DPI measured concentrations (fmol $cell^{-1}$ ± 1s)

[b] trace amounts detected

Table S2. Fatty acid components of IPLs from CCMP 374, EhV86-infected CCMP 374 and EhV86

| | | *Ehux374* (% of lipidome) | | | | | 4-DPI *Ehux374* (% of lipidome) | | | | | EhV86 |
|---|---|---|---|---|---|---|---|---|---|---|---|---|
| Class | Fatty Acids | 0 d | 1 d | 2 d | 3 d | 4 d | 0 d | 1 d | 2 d | 3 d | 4 d | (%) |
| MGDG | 14:0/14:0 | 0.6 | 0.7 | 0.8 | 0.4 | 0.4 | 0.7 | 0.5 | 0.2 | 0.4 | 0.2 | 0.0 |
| | 14:0/18:1 | 2.0 | 2.3 | 1.4 | 0.8 | 0.7 | 2.0 | 2.3 | 1.8 | 0.9 | 1.2 | 0.6 |
| | 14:0/18:4 | 6.3 | 5.7 | 4.1 | 2.3 | 1.7 | 6.1 | 3.9 | 0.7 | 0.4 | 0.4 | 0.0 |
| | 14:0/18:5 | 3.4 | 2.6 | 2.4 | 1.4 | 0.9 | 2.8 | 2.8 | 1.1 | 0.4 | 0.2 | 0.0 |
| | 18:4/18:4 | 4.6 | 4.9 | 3.6 | 2.9 | 2.0 | 4.8 | 2.9 | 1.4 | 0.9 | 0.4 | 0.0 |
| | 18:4/18:5 | 7.1 | 8.1 | 8.1 | 7.2 | 6.6 | 7.4 | 6.4 | 4.9 | 3.2 | 0.6 | 0.0 |
| | 18:5/18:5 | 8.2 | 8.9 | 13.3 | 14.9 | 17.3 | 7.9 | 12.7 | 11.5 | 6.7 | 1.3 | 0.0 |
| | 18:5/22:6 | 0.8 | 0.8 | 0.8 | 1.2 | 0.9 | 0.9 | 0.6 | 0.7 | 0.4 | 0.4 | 0.0 |
| | 22:6/22:6 | 1.5 | 1.3 | 1.2 | 1.2 | 1.1 | 1.2 | 0.9 | 0.7 | 0.4 | 0.2 | 0.0 |
| DGDG | 14:0/14:0 | 1.4 | 1.2 | 0.6 | 0.5 | 0.5 | 1.5 | 1.1 | 0.5 | 0.4 | 0.8 | 0.0 |
| | 14:0/18:1 | 3.9 | 3.0 | 1.5 | 1.0 | 0.9 | 3.9 | 2.8 | 2.2 | 1.9 | 1.3 | 0.0 |
| | 14:0/18:4 | 1.2 | 0.8 | 0.3 | 0.1 | 0.1 | 1.2 | 0.8 | 0.2 | 0.2 | 0.2 | 0.0 |
| | 14:0/18:5 | 0.9 | 0.8 | 0.5 | 0.3 | 0.1 | 0.7 | 0.6 | 0.4 | 0.2 | 0.2 | 0.0 |
| | 18:5/18:5 | 11.2 | 10.6 | 12.5 | 16.1 | 17.3 | 10.9 | 11.1 | 8.6 | 2.6 | 1.3 | 0.0 |
| SQDG | 14:0/14:0 | 3.2 | 2.9 | 2.0 | 2.5 | 2.5 | 3.8 | 3.3 | 4.3 | 6.2 | 9.2 | 0.0 |
| | 14:0/16:0 | 1.2 | 1.2 | 0.8 | 1.0 | 1.1 | 1.3 | 1.3 | 1.6 | 3.2 | 3.7 | 0.0 |
| | 14:0/18:3 | 7.6 | 6.8 | 5.4 | 5.9 | 5.1 | 8.3 | 7.7 | 6.8 | 4.7 | 1.7 | 0.0 |
| | 14:0/18:4 | 1.2 | 0.9 | 0.8 | 1.0 | 0.9 | 1.0 | 1.0 | 1.4 | 1.3 | 0.4 | 0.0 |
| | 14:0/22:6 | 2.2 | 2.1 | 1.4 | 1.6 | 1.7 | 2.5 | 2.0 | 2.3 | 2.4 | 1.2 | 0.0 |
| | 18:3/18:4 | 4.6 | 4.6 | 4.1 | 5.4 | 5.9 | 4.8 | 5.3 | 5.4 | 2.6 | 0.6 | 0.0 |
| PC | 14:0/22:6 | 2.0 | 2.1 | 2.0 | 1.5 | 1.3 | 1.9 | 2.1 | 2.2 | 1.7 | 0.8 | 0.3 |
| | 16:0/22:6 | 0.3 | 0.3 | 0.3 | 0.3 | 0.4 | 0.3 | 0.3 | 0.4 | 0.4 | 0.4 | 0.1 |
| | 18:1/22:6 | 0.3 | 0.3 | 0.2 | 0.3 | 0.3 | 0.3 | 0.4 | 1.1 | 1.1 | 0.6 | 0.4 |
| | 22:6/22:6 | 3.1 | 3.3 | 4.4 | 3.7 | 3.7 | 2.9 | 3.2 | 4.3 | 4.5 | 1.2 | 0.7 |
| PDPT | 14:0/22:6 | 7.6 | 9.0 | 10.9 | 10.1 | 9.3 | 7.1 | 7.7 | 7.0 | 4.9 | 2.7 | 1.0 |
| | 16:0/22:6 | 1.2 | 1.5 | 1.7 | 1.6 | 1.7 | 1.3 | 1.1 | 1.4 | 1.5 | 1.0 | 0.3 |
| | 18:1/22:6 | 0.9 | 0.8 | 0.9 | 0.8 | 0.9 | 0.9 | 0.9 | 2.9 | 3.4 | 1.2 | 0.6 |
| | 22:6/22:6 | 1.7 | 1.9 | 2.4 | 2.3 | 2.1 | 1.9 | 1.9 | 2.5 | 2.8 | 1.2 | 0.4 |
| PG | 16:2/20:5 | 0.6 | 0.5 | 0.6 | 0.5 | 0.5 | 0.6 | 0.6 | 0.4 | 0.2 | 0.2 | 0.0 |
| PE | 14:0/16:1 | 0.0 | 0.0 | 0.0 | 0.0 | 0.0 | 0.0 | 0.0 | 0.2 | 0.9 | 2.3 | 0.0 |
| | 15:0/16:1 | 0.0 | 0.0 | 0.0 | 0.0 | 0.0 | 0.1 | 0.1 | 0.4 | 1.9 | 6.2 | 0.0 |
| | 16:0/16:1 | 0.0 | 0.0 | 0.0 | 0.0 | 0.0 | 0.0 | 0.0 | 0.2 | 1.3 | 4.0 | 0.1 |
| | 17:0/16:1 | 0.0 | 0.0 | 0.0 | 0.0 | 0.0 | 0.0 | 0.0 | 0.0 | 0.2 | 1.2 | 0.8 |
| | 18:0/16:1 | 0.0 | 0.0 | 0.0 | 0.0 | 0.0 | 0.0 | 0.0 | 0.0 | 0.0 | 1.3 | 0.5 |
| DGCC | 14:0/22:6 | 2.6 | 4.0 | 4.4 | 4.4 | 4.8 | 2.5 | 3.8 | 2.7 | 2.1 | 1.3 | 1.2 |
| | 16:0/22:6 | 0.3 | 0.5 | 0.5 | 0.5 | 0.5 | 0.3 | 0.4 | 0.5 | 0.9 | 0.4 | 0.3 |
| | 18:1/22:6 | 0.2 | 0.1 | 0.2 | 0.3 | 0.1 | 0.1 | 0.3 | 0.7 | 1.1 | 0.2 | 0.4 |
| | 22:6/22:6 | 1.1 | 1.3 | 1.8 | 1.6 | 1.7 | 1.0 | 1.4 | 1.4 | 1.5 | 0.4 | 0.6 |
| BLL | 14:0/22:6 | 0.0 | 0.0 | 0.0 | 0.0 | 0.0 | 0.0 | 0.4 | 2.5 | 2.1 | 0.4 | 0.5 |
| | 16:0/22:6 | 0.9 | 0.9 | 0.9 | 1.0 | 0.8 | 0.9 | 0.8 | 0.2 | 0.2 | 0.2 | 0.1 |
| | 18:1/22:6 | 0.6 | 0.5 | 0.6 | 0.7 | 0.7 | 0.7 | 0.6 | 0.4 | 0.4 | 0.2 | 0.2 |
| | 22:6/22:6 | 0.0 | 0.0 | 0.0 | 0.0 | 0.0 | 0.0 | 0.0 | 0.2 | 0.6 | 0.8 | 4.0 |
| DGTS | 14:0/18:1 | 0.6 | 0.5 | 0.6 | 0.5 | 0.5 | 0.6 | 0.6 | 1.4 | 3.6 | 4.0 | 1.0 |
| | 14:0/18:4 | 0.2 | 0.1 | 0.2 | 0.3 | 0.3 | 0.1 | 0.3 | 0.2 | 0.2 | 0.2 | 0.0 |
| | 18:1/22:6 | 0.3 | 0.3 | 0.2 | 0.1 | 0.3 | 0.3 | 0.3 | 0.4 | 1.3 | 1.5 | 0.1 |
| | 18:4/22:6 | 0.2 | 0.0 | 0.0 | 0.0 | 0.0 | 0.0 | 0.0 | 0.4 | 0.2 | 1.3 | 0.1 |
| hGSL | 22:3, 22:2 | 0.9 | 0.8 | 1.1 | 0.8 | 0.9 | 0.9 | 1.0 | 1.6 | 2.4 | 1.2 | 7.2 |
| vGSL | 22:0[a] | 0.2 | 0.0 | 0.2 | 0.1 | 0.1 | 0.1 | 0.5 | 5.9 | 14.4 | 30.4 | 63.5 |
| sGSL | 22:0 | 1.1 | 1.1 | 1.1 | 1.0 | 1.1 | 1.3 | 1.5 | 1.6 | 4.5 | 8.1 | 15.0 |

[a] vGSL includes species with C18, C19, C20, C21, C22, C23, and C24 saturated and monounsaturated fatty acids

Table S3. Glycosphingolipid content of E. huxleyi strains in culture

| Strain | EhV1[a] | EhV86[a] | EhV163[a] | sGSL (fmol cell$^{-1}$) | hGSL (fmol cell$^{-1}$) | sGSL/hGSL[b] |
|---|---|---|---|---|---|---|
| CCMP 373 | R | R | R | -[c] | 0.08 | 0.00 |
| CCMP 374 | S | S | S | 0.07 | 0.06 | 1.10 |
| CCMP 379 | | R | R | - | 0.43 | 0.00 |
| CCMP 1516 | S | S | S | 0.02 | 0.06 | 0.34 |
| CCMP 2090 | S | S | R | 0.02 | 0.09 | 0.18 |
| DHB 601 | | | | n.d.[d] | 0.08 | 0.03 |
| DHB 604 | | | | n.d. | 0.03 | 0.10 |
| DHB 606 | R | R | R | n.d. | 0.14 | 0.04 |
| DHB 607 | | | | - | 0.08 | 0.00 |
| DHB 610 | | | | - | 0.08 | 0.00 |
| DHB 611 | S | S | S | 0.13 | 0.08 | 2.46 |
| DHB 613 | | | | - | 0.05 | 0.00 |
| DHB 615 | R | R | R | n.d. | 0.03 | 0.20 |
| DHB 621 | | | | n.d. | 0.04 | 0.12 |
| DHB 623 | S | S[e] | S | 0.02 | 0.08 | 0.09 |
| DHB 624 | | | | 0.33 | 0.23 | 2.45 |
| DHB 626 | | | | - | 0.05 | 0.00 |
| DHB 629 | R | R | R | - | 0.04 | 0.00 |
| DHB 630 | | | | n.d. | 0.05 | 0.01 |
| DHB 639 | | | | 0.04 | 0.03 | 1.65 |
| DHB 641 | R | R | R | n.d. | 0.12 | 0.08 |
| DHB 645 | | | | 0.14 | 0.11 | 1.57 |
| DHB 648 | | | | - | 0.06 | 0.00 |
| DHB 650 | | | | 0.05 | 0.06 | 0.77 |
| DHB 655 | | | | - | 0.21 | 0.00 |
| DHB 657 | | | | 0.07 | 0.06 | 1.52 |
| DHB 659 | | | | 0.13 | 0.10 | 2.55 |

[a] *E. huxleyi* strains characterized as sensitive (S) or resistant (R) to EhV infection.

[b] ratio calculated based on MS response (peak areas).

[c] sGSL not detected.

[d] not determined. sGSL was detected below the limit of quantitation.

[e] slight sensitivity with growth impeded by no virus production observed.

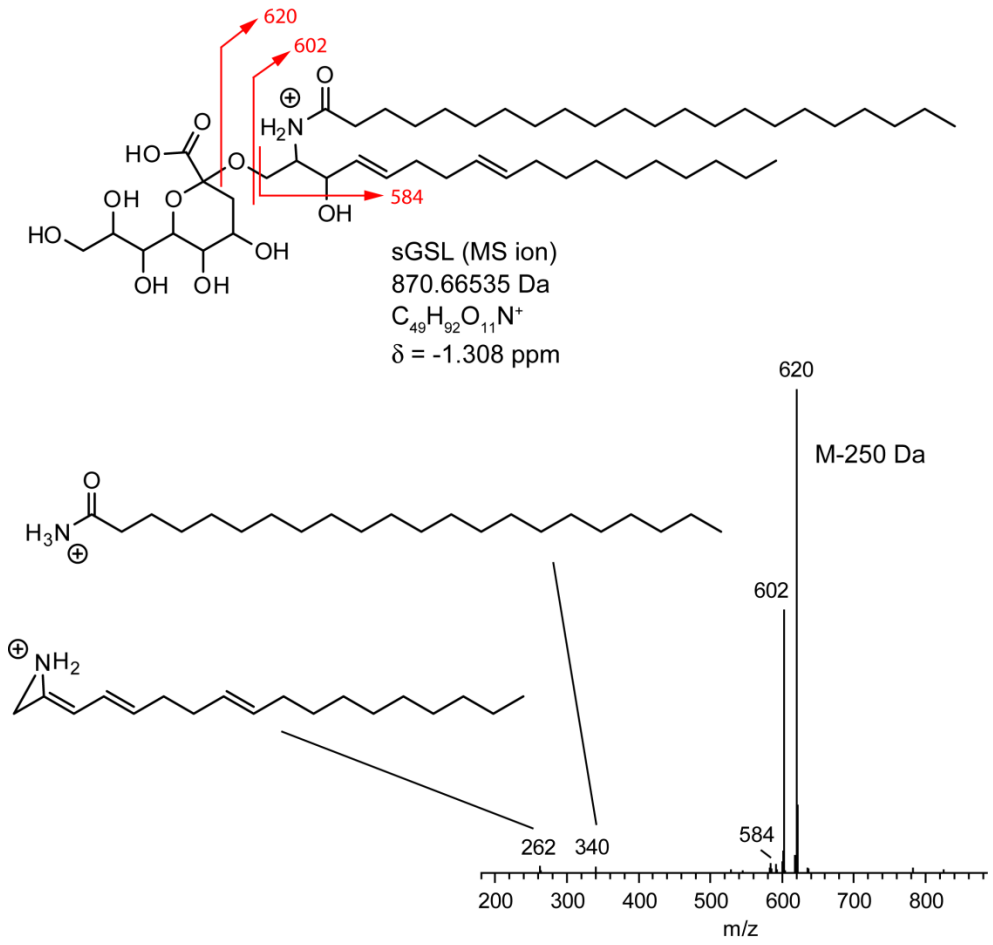


Figure S1. Ion trap $MS^2$ positive ion mass spectrum of the m/z 870 sGSL molecular ion. The $MS^2$ mass spectrum of sGSL is similar to other glycosphingolipids, with headgroup and water neutral losses accounting for the m/z 620, 602, and 584 ions. The major neutral losses of 268 and 250 Da reveal that the headgroup is larger than a simple sugar. The m/z 340 and 262 $MS^2$ ions indicate that sGSL has a C22:0 fatty acid and d18:2 long chain base. Accurate mass determination by FT-ICR-MS showed that the molecular ion has m/z 870.66535, supporting a molecular formula of $C_{49}H_{92}O_{11}N^+$ (δ = -1.308 ppm), and that the main $MS^2$ ions have m/z 620.59733 ($C_{40}H_{78}O_3N^+$; δ = -0.470 ppm), m/z 602.58694 Da ($C_{40}H_{76}O_2N^+$; δ = -0.194 ppm), m/z 584.57937 ($C_{40}H_{74}ON^+$; δ = 4.922 ppm) and m/z 262.25294 ($C_{18}H_{32}N^+$; δ = 0.051 ppm). We did not detect the 340 Da amino fatty acid by high resolution MS. The headgroup neutral loss (870.66535 - 602.58694 = 268.07841 Da) supports the formula $C_9H_{16}O_9$ (δ = -1.766 ppm), which is the same as the sialic acid 2-Keto-3-deoxynonic acid (Kdn).

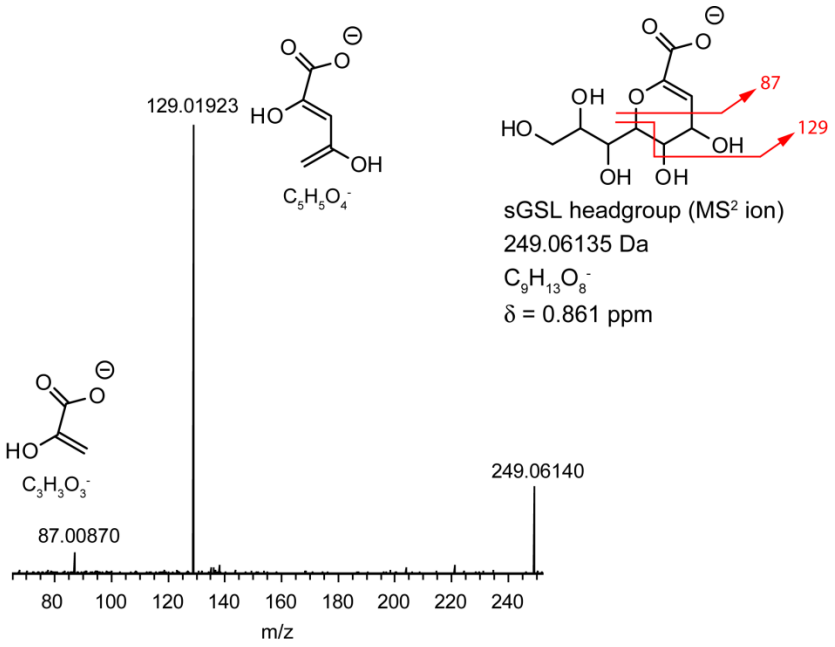


Figure S2. FT-ICR-MS $MS^3$ negative ion mode mass spectrum of the sGSL headgroup. In negative ion mode, sGSL was detected with m/z 868.65134 ($C_{49}H_{90}O_{11}N^-$, δ = 0.557 ppm). The $MS^2$ product ion with m/z 249.06140 supports a formula of $C_9H_{13}O_8^-$ (δ = 0.861 ppm), which suggests the retention of the ether linking oxygen on ceramide and the transfer of hydrogen from the negative ion and the subsequent C=C double bond formation. The most abundant $MS^3$ fragment ions have m/z 129.01923 ($C_5H_5O_4^-$, δ = 7.711 ppm) and m/z 87.00870 ($C_3H_3O_3^-$, δ = 11.832). Their requirement of three and two double bonds, respectively, suggests that they most likely include the carboxyl moiety and derive from ring cleavage.

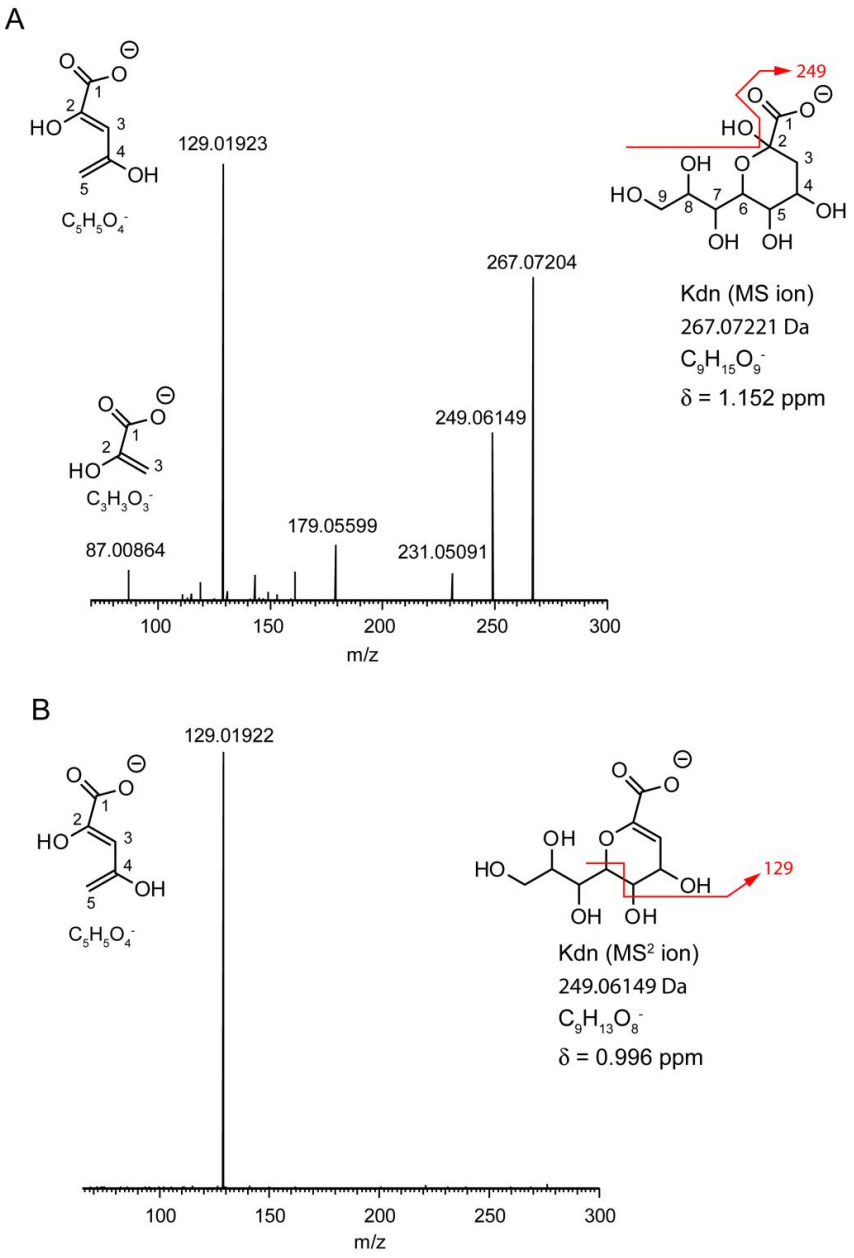


Figure S3. FT-ICR-MS $MS^2$ and $MS^3$ negative ion mode mass spectra for 2-Keto-3-deoxynonic acid (KDN). Panel A is the $MS^2$ spectrum of the m/z 267.07221 MS parent ion, showing two water losses (m/z 249.06149 and 231.05091) and m/z 129.01923 and 87.00864 ions similar to those in the sGSL $MS^3$ spectrum (Fig. S2). The m/z 249.06149 ion likely results from dehydration at the $C_2$ position with a double bond formed between $C_2$ and $C_3$. Panel B is the $MS^3$ spectrum of the m/z 249.06149 $MS^2$ ion, which is dominated by a m/z 129.01922 product, similar to the sGSL $MS^3$ spectrum in figure S2, supporting our assignment of the single sialic acid KDN headgroup for sGSL.

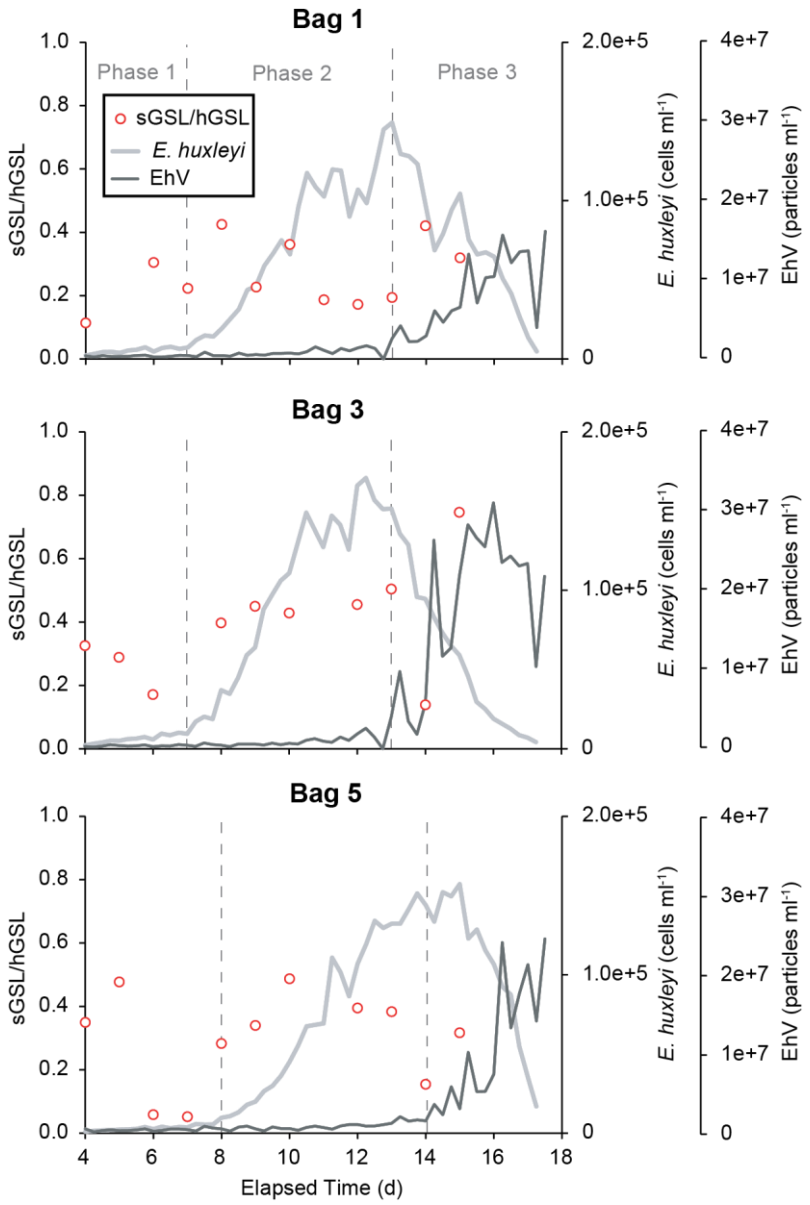


Figure S4. Ratios of sGSL/hGSL in mesocosm bags 1, 3, and 5. Growth phase 1 is lag phase, phase 2 is exponential growth and phase 3 includes *E. huxleyi* demise and EhV proliferation.